Received: 22 January 2024 | Revised: 15 April 2024 | Accepted: 25 April 2024

DOI: 10.1002/oa.3305

RESEARCH ARTICLE

A new laboratory-based method to experimentally induce diagenetic modifications in human bone tissue using archaeological gravesoils

Valentina Caruso[1,2] | Nicoletta Marinoni[1] | Valeria Diella[3] | Elena Ferrari[1] | Elena Possenti[4] | Luca Trombino[1] | Cristina Cattaneo[2] | Alberto Viani[5]

[1]Dipartimento di Scienze della Terra "Ardito Desio,", Università degli Studi di Milano, Milan, Italy

[2]LABANOF, Laboratorio di Antropologia e Odontologia Forense, Sezione di Medicina Legale e delle Assicurazioni, Dipartimento di Scienze Biomediche per la Salute, Università degli Studi di Milano, Milan, Italy

[3]Consiglio Nazionale delle Ricerche, IGAG, Sezione di Milano, Milan, Italy

[4]Consiglio Nazionale delle Ricerche, ISPC, Sezione di Milano, Milan, Italy

[5]Dipartimento di Scienze Chimiche e Geologiche, Università degli Studi di Modena e Reggio Emilia, Modena, Italy

Correspondence
Caruso Valentina and Marinoni Nicoletta, Dipartimento di Scienze della Terra "Ardito Desio," Università degli Studi di Milano, via Luigi Mangiagalli 34, 20133 Milano, Italy.
Email: caruso.valentina87@gmail.com and nicoletta.marinoni@unimi.it

Funding information
This work was supported by Fondazione Fratelli Confalonieri, Milan (Italy).

[Correction added on 23 May 2024, after online publication: The first and last name of the authors have been corrected in this version.]

Abstract

The conditions of the burial environment trigger microstructural modifications and physical-chemical changes in the bone, such as chemical dissolution, increase of crystallinity, chemical exchanges, collagen degradation and changes in porosity, hence to reproduce these patterns is a challenging task. This work presents a new method to accelerate the diagenetic processes in the laboratory. Artificial aging is obtained by immersion at 80°C in "enriched" solutions derived from the leaching of gravesoils, maintaining the same pH, for 1 month, on modern bones collected from an autopsy. Two distinct solutions from two graves of the necropolis of Travo (IT) (7th–8th century AD) were adopted. The induced damage patterns, on the bone microstructure and the organo-mineral fraction, have been compared with those observed on buried skeletal elements from the same graves, by providing a multi-analytical approach (BSE-SEM, EMPA, FT-IR, MP-AES). Bioapatite parameters, such as crystallinity index and Ca/P molar ratio, evolved similarly and, in some cases, reached the same values of buried bones. Conversely, in the absence of microbial activity, the organic fraction better survived the artificial aging. For the same reason, the porosity due to bioerosion was absent in the artificially aged samples, whereas the biological pores and the post-mortem fractures exhibited the same histomorphology. It is believed that the opportunity of reproducing the diagenetic changes by replicating the chemical environment of the burial site at the laboratory scale is of great interest to forensic science and archaeology (e.g., to reconstruct the burial environment).

KEYWORDS
bone porous microstructure, burial soil geochemistry, laboratory-induced bone diagenesis, multi-analytical bone characterization, necropolis of Travo, organo-mineral bone preservation

1 | INTRODUCTION

Bone is a highly specialized connective tissue, with an organo-mineral hierarchical organization, undergoing physical, chemical, and biological post-mortem modifications. After death, mostly owing to the activity of microorganisms, the organic fraction is degraded by collagen hydrolysis (Child, 1995; Collins et al., 2002; Hedges, 2002), resulting in the opening of fibrous collagen proteins, which favors the dissolution of the

inorganic fraction, carbonate-hydroxyapatite (CHA) (Keenan, 2016; Keenan et al., 2015). The chemical dissolution of the mineral fraction exposes the organic matrix to the attack of microbes, promoting the degradation of proteins (Collins et al., 2002). However, bioapatite can recrystallize in a more thermodynamically stable form over time under a range of pH conditions (7.8–8) (Berna et al., 2004).

The extent of bone degradation depends both on intrinsic factors (composition, species, biological age) and on several extrinsic factors (type of burial, post-depositional history, burial environment). In particular, temperature, pH, type of sediment, soil geochemistry, water, and so forth play a key role in dictating the state of preservation of skeletal remains in the archaeological and forensic records (Caruso et al., 2020, and references therein).

Experimental studies have been performed at the laboratory scale using animal bones to test the influence of the environment on bone degradation. Behrensmeyer (1978) exposed, for over 12 years, animal carcasses in buried and sub-aerially conditions to explore their overall susceptibility to physical and compositional degradation, with respect to the soil/water environment. The recorded bone weathering rate provided clues to characterize the archaeological sites, with respect to the deposition conditions (such as duration of occupation, condition of burial, and presence of non-cultural bone material). Later, similar experiments using animal carcasses, in a series of controlled buried and unburied scenarios (i.e., climate-controlled greenhouse environment), have been conducted to monitor changes in the mineral crystallinity and the histological integrity of bones, mainly induced by bacterial bioerosion, over a period ranging from 6 months (Boaks et al., 2014; Fisk et al., 2019; Krajcarz, 2019; Walden et al., 2018; White & Booth, 2014) up to 40 years (Fernández-Jalvo et al., 2010; Kontopoulos et al., 2016; Trueman et al., 2004). In the early post-mortem period (<1 year), White and Booth (2014) demonstrated that the survival of bone biomolecules and the histological integrity of bones mainly depend upon the mechanisms of skeletonization. Also, Fisk et al. (2019) asserted that the compositional and physical changes in buried skeletons may vary according to the maturity of bones. Walden et al. (2018) claimed that the elemental concentration of bone traced the original sediment in which skeletons were deposited. Moreover, Boaks et al. (2014) and Krajcarz (2019) demonstrated that the concentration of selected chemical elements in bone and the degree of deterioration of collagen may be used to predict the time since death (i.e., the post-mortem interval; PMI) in case of human remains with unknown date of deposition. Recently, Mein and Williams (2023) presented a novel method for PMI estimation by counting normal versus diagenetic osteocyte lacunae within the microstructure of the bone. The authors recorded evidence of altered osteocyte lacunae in a short post-mortem period (<4 weeks) and highlighted the crucial role played by intrinsic gut microbiota and depositional environment (soil vs. surface decomposition) on bone bioerosion. Long-term studies of bone degradation indicated that bones in contact with the soil undergo rapid and extensive mineralogical and chemical alteration, including the growth of bioapatite crystallites and the precipitation of authigenic minerals, facilitated by the decomposition of the organic matrix (Trueman et al., 2004). Otherwise, the alterations induced by the environmental agents on the mineral compartment of bone and on collagen proteins after death are difficult to identify (Fernández-Jalvo et al., 2010). Moreover, the macroscopic appearance and microscopic preservation of bones may be significantly different, since every skeletal element may follow a unique diagenetic trajectory, because of their biomechanical characteristics, age, diseases, and so forth (Kontopoulos et al., 2016).

Laboratory-based degradation experiments under acidic conditions on modern and archeological animal bones (High et al., 2015) indicated that the loss of bone minerals is accelerated at low pH and leads to the increased breakdown of the bone collagen; a process hastened in archaeological samples. Similar experiments have been rarely conducted on human cadavers, even if the histological microarchitectures and the distribution of organic and inorganic components differ in bones from different species, leading to diverse diagenetic trajectories (Kendall et al., 2018). Delannoy et al. (2016) employed defleshed bone fragments sampled from autopsied individuals. They tested the loss of bone mass for 90 days to predict the PMI, according to burial locations and conditions in which they were placed. Their results proved that the study of the effects of diagenesis, defined as all cumulative physical, chemical, and biological processes that alter the bone tissue in the burial environment (Guarino et al., 2006), may provide valuable information on the history of bones, in terms of the local burial environment and anthropogenic practices.

In this scenario, the current study presents the potential of a new laboratory-based method to artificially induce degradation in human bones during a short period (1 month), to replicate the bone deterioration effects observed in the archaeological record and caused by the contact with the burial soil. Fresh bones were sampled from an autopsied individual and were aged by immersion in solutions obtained from the leaching of two distinct soils from burials of the same archaeological site.

Since the "time-factor" is crucial when performing aging experiments (High et al., 2015), the bone degradation kinetics were accelerated by performing the experiments at 80°C, maintaining the same conditions of pH observed in the original gravesoils.

The proposed methodology was validated by comparing the artificially induced modifications with those recorded in the archaeological bones buried in the soil from which the leachates were obtained. A multi-analytical approach was adopted for histological, mineralogical, and chemical analysis of the bones, the conditioning solutions, and the gravesoils.

This innovative and preliminary approach attempts to overcome some limitations of the abovementioned experiments, since it (i) is not too time-consuming, (ii) can be performed at the laboratory scale, (iii) requires a minimal sample preparation, (iv) is reproducible, and (v) involves an easy and fast data collection procedure. For these reasons, this approach can be extended to further research cases, in the light of gaining a better understanding of the role played by the different diagenetic processes in the preservation of the bone tissue, thanks to the possibility of recreating different post-mortem scenarios and environmental conditions at the laboratory scale.

2 | MATERIAL

2.1 | Buried bones from the necropolis of Sant'Andrea, Travo (IT)

The studied area is in the territory of Travo (Italy), in the Trebbia Valley, on the Western Apennines, at 170 m above sea level, on the left bank of the Trebbia River. Travo is located where the lithotypes of Luretta Valley merge, NO-SE orientated to the Apennine mountain chain. This formation is constituted by two lithostratigraphic units dated from Upper Pliocene to Middle Eocene. Sedimentary lithotypes characterize the area made of debris, conglomerates, sandstones, siltstones, argillites, marls, limestones, and jaspers. Igneous and metamorphic rocks are also frequently found. Moreover, as superficial deposits, fluvial materials derived from recent and present-day alluvial deposits can be observed. The studied gravesoils are mainly vertisols, produced by weathering of the clay-rich parent material during the wet and dry seasons.

The necropolis of Sant'Andrea was discovered in 2005, and 117 tombs, mainly earthy pits, for a total surface area of 545 m^2, dated from the 7th to 8th century AD (Conversi & Mezzadri, 2011), have been excavated. Most of the human inhumations recovered were deposited in single tombs in supine position and belonged to adult individuals. Two tombs, numbered 17 and 50 (hereafter reported as T17 and T50, respectively), which preserved the remains of entire skeletons of male adult individuals (30–50 years old; Brooks & Suchey, 1990 and Buikstra & Ubelaker, 1994), were selected. The samples used in this study were obtained by cutting two transverse sections from one femur for each individual. Femora were selected for a PhD project (Caruso, 2017) and then used here for their availability and high conservation in the ground, compared with other skeletal elements.

As reported in Table 1, the buried bones are labeled B as buried bone, followed by the tomb number (i.e., B17 means buried bone from T17). Similarly, the gravesoil samples are labeled G as gravesoil, followed by the number of the tomb (i.e., G17 means gravesoil of T17).

2.2 | Fresh bones

The fresh human bones were obtained from two skeletal elements of one single adult male autopsied individual (38 years old) at the Institute of Legal Medicine of Milan (Italy), according to Police Mortuary Regulations (DPR 285/90 art. 43). During autopsy, two different anatomical skeletal regions are always sectioned and studied, namely, skull and rib cage; hence, because of their availability, they were selected for this study.

One section of the cranium and rib was collected during the forensic autopsy. Then, each one was split into seven pieces of similar size (approximately 1 × 1 × 1 cm) using a diamond-coated low-speed rotary saw and immediately manually defleshed. Another section of the cranium and rib was initially left untreated to be used as a control.

The fresh bones used as control are labeled: C for cranium and R for rib (Table 1).

The skeletal elements collected for the aging experiment differed from the ones of archaeological provenance, because of the availability of the bone material, as specified above. However, the biological age was kept the same (see Table 1), to minimize the differences in terms of collagen content and chemical composition at death. According to Crowder and Stout (2011), cranial, rib, and femur bones are comparable for histology, mineral, chemical, and collagen assessment, and these parameters seem to evolve similarly during the diagenesis irrespective of the type of bone (Margariti et al., 2019; Rogoz et al., 2012).

3 | METHODS

3.1 | Aging test

The two fragments of fresh cranium and rib were immersed into two "enriched" solutions with the chemical elements extracted from the gravesoils of T17 and T50, to simulate the natural decomposition process.

The "enriched" solutions were obtained as follows: 10 g of gravesoil for each tomb was treated with 25 mL of demineralized water (pH 8.36) for 48 h, and then the residue was filtered. These "enriched" solutions were used for the laboratory-based-degradation experiment, and their pH, measured after the preparation, was found to be 7.98, similar to one of the gravesoils. Demineralized water was used in the experiment to replicate natural atmospheric precipitations. The chemical changes that occurred before and after the experiment in the "enriched" solutions were monitored by the Microwave plasma–atomic emission spectrometry (MP-AES).

In Table 1 the labeling of the "enriched" solution and the aged bone is summarized. The "enriched" solutions kept as control are labeled S, as a solution, followed by the number of the tomb from which the gravesoil comes (i.e., S17 means solution derived from the leaching of the gravesoil of T17). Instead, the "enriched" solutions left in contact with the bones for 30 days, generally named aged solutions, are labeled as follows: XYZ_K where X = S, solution; Y = A, aged; Z = 17 or 50, for S17 and 50, respectively; _K = C or R for cranium and rib, respectively (i.e., SA17_C means solution S17 aged with the cranium).

After the preparation of the "enriched solutions," two pieces of fresh cranium and rib were immersed in 4 mL of each solution in sealed PFA containers and then placed in an oven at 80°C (High et al., 2015) for 1 month. This should accelerate the deterioration process, since the heating should increase the reaction/degradation rates concerning those expected at room temperature. The samples were extracted at 15 and 30 days, and the mineralogical and chemical composition of bones was determined by employing electron microprobe analysis (EMPA) and Fourier transform infrared spectroscopy (FT-IR).

These so-called aged bones are labeled as follows (Table 1): XYZ_K, where X = C or R for a fragment of cranial and rib bone, respectively; Y = A, aged; Z = 17 or 50, for S17 or S50, respectively; _K = 15 or 30, for the days left from the beginning of the test (i.e., CA17_15 means cranium aged, immersed in S17 for 15 days).

TABLE 1 Information on experimental conditions is provided for every sample, labeled with different ID codes.

Bone sample ID	Description	Age/provenance	Biological age at death/sex	pH	Temperature (°C)	Time elapsed of aging test (days)	Gravesoil
Control samples							
C	Cranium fresh (control)	Present/Autopsy	38/male	-	Room	0	-
R	Rib fresh (control)			-	Room	0	-
Aged samples							
CA17_15	Cranium aged left in S17 for 15 days	Present/Autopsy	38/male	8	80	15	Tomb 17
CA17_30	Cranium aged left in S17 for 30 days			8	80	30	Tomb 17
CA50_15	Cranium aged left in S50 for 15 days			8	80	15	Tomb 50
CA50_30	Cranium aged left in S50 for 30 days			8	80	30	Tomb 50
RA17_15	Rib aged left in S17 for 15 days			8	80	15	Tomb 17
RA17_30	Rib aged left in S17 for 30 days			8	80	30	Tomb 17
RA50_15	Rib aged left in S50 for 15 days			8	80	15	Tomb 50
RA50_30	Rib aged left in S50 for 30 days			8	80	30	Tomb 50
Archaeological samples							
B17	Buried bone from T17	7^{th}–8^{th} century AD/ Necropolis of Travo	30–50/male	8	-	-	Tomb 17
B50	Buried bone from T50			8	-	-	Tomb 50
Gravesoil ID	**Description**	**Age/Provenance**		**pH**			**Gravesoil**
G17	Gravesoil of Tomb 17	7^{th}–8^{th} century AD/ Necropolis of Travo		7.38	-	-	Tomb 17
G50	Gravesoil of Tomb 50	7^{th}-8^{th} century AD/ Necropolis of Travo		8	-	-	Tomb 50
Solution ID	**Description**			**pH**	**Temperature (°C)**	**Time elapsed of aging test (days)**	**Gravesoil**
S17	Solution that derived from the leaching of the gravesoil of T17 (control)			8	Room	0	Tomb 17
S50	Solution that derived from the leaching of the gravesoil of T50 (control)			8	Room	0	Tomb 50
SA17_C	Solution aged that derived from the leaching of the gravesoil of T17 and left for 30 days in contact with cranium			8	80	30	Tomb 17
SA17_R	Solution aged that derived from the leaching of the gravesoil of T17 and left for 30 days in contact with rib			8	80	30	Tomb 17
SA50_C	Solution aged that derived from the leaching of the gravesoil of T50 and left for 30 days in contact with cranium			8	80	30	Tomb 50
SA50_R	Solution aged that derived from the leaching of the gravesoil of T50 and left for 30 days in contact with rib			8	80	30	Tomb 50
SG17	Solution of the gravesoil of T17			8	-	-	Tomb 17
SG50	Solution of the gravesoil of T50			8	-	-	Tomb 50

3.2 | Gravesoils analysis

3.2.1 | Physical analysis

Particle size analysis of gravesoil was performed using 100 g of the fine earth fraction obtained by one or more subsequent quartering. The obtained fraction was weighed and then pre-treated with hydrogen peroxide (H_2O_2, 130 v/v) to destroy the organic matter, which, by favoring aggregate formation, could interfere with the analysis. Two distinct methodologies were employed to characterize different granulometric fractions: the sand fraction (particles of diameter varying between 2 mm and 63 μm) was determined by sieving, whereas the silt fraction (particles of diameter varying 63 and 2 μm) was determined by the Casagrande aerometer method (Avery, 1974; Gale & Hoare, 1991). The amount of clay was deduced by subtracting the sands and silts from the initial weight of the sample.

The pH was determined in distilled water, using the sample sieved to 2 mm. For each sample, 10 g of gravesoil was added to 25 mL of solution (proportion gravesoil/solution of 1/2.5); the suspension was placed on a shaker for 20 min and then left to stand for 24 h. The pH measurement was carried out using an automatic dual-point calibration tester.

Organic carbon determination of the original representative sample was obtained through the standard method by Walkley and Black (1934), which uses the reduction of potassium dichromate $K_2Cr_2O_7$ excess by organic matter and the subsequent determination of the remaining $K_2Cr_2O_7$ by oxide-reductive titration iron with a solution of iron ammonium sulfate. The weight of the samples was approximately 0.250 g.

3.2.2 | Chemical analysis with MP-AES

MP-AES was used to analyze the gravesoils. Samples were prepared as follows: after sieving the fine earth fraction, in quantities of about 100 g, T17 and T50 gravesoils were quartered to obtain two homogeneous representative sub-samples. Samples were prepared in duplicate: 0.1 g of each sub-sample was weighted and suspended in 0.5 mL of hydrogen peroxide (H_2O_2) to enhance the destruction of organic matter. Then, aqua regia, prepared with a mixture of 0.5 mL of nitric acid (HNO_3, 60% v/v) and 1.5 mL of hydrochloric acid (HCl, 37% v/v), was added and the four sub-samples were heated at 80°C for 2 h. Aqua regia, although considered adequate for "total" trace element determination, only provides a "partial" extraction for most rock-forming elements and more refractory elements (e.g., Cd, Cu, Pb, Zn, Cr, Ni, and Ba) (Gaudino et al., 2007). After digestion, each sub-sample was transferred to a volumetric flask and diluted with ultrapure water to 25 mL before analysis.

The solutions of the gravesoils were labeled SG, as the solution of gravesoil, followed by the number of the tomb, 17 or 50 (i.e., SG17 means the solution of gravesoil of T17).

The solutions of gravesoil (SG), together with the solutions prepared and used for the aging experiment, that is, the "enriched" solutions left as control (S) and the "enriched" solution aged with bones (SA), were analyzed using an Agilent 4100 Microwave Plasma spectrometer (MP-AES). The instrument was calibrated using three multi-element standard solutions at different concentrations.

3.2.3 | X-ray powder diffraction (XRPD)

The analysis was conducted on the original gravesoils and the residue of gravesoils after the preparation of the solutions. A few micrograms of material were ground by hand, side loaded on a flat Al sample-holder, and measured with a PANalytical X'Pert diffractometer in Bragg–Brentano geometry, using CuKα radiation (1.5417 Å) at 40 kV and 40 mA. The diffracted intensity was collected on an X'Celerator detector, over the angular range of 5°–80° 2θ. Divergence slits of 1/2° were placed on the incident beam, and 0.1 mm receiving slits were placed on the diffracted beam. The XRPD patterns were collected with a counting time of 30 s/step with a 0.01° 2θ step. The XRPD qualitative analysis was performed by means of the PANalytical X'Pert HighScore software. Rietveld refinement (Young, 1993) was performed on diffraction patterns using the GSAS-II program to obtain the weight fraction of the mineral phases.

3.2.4 | Scanning electron microscopy with an energy-dispersive X-ray analyzer (SEM-EDS)

SEM-EDS provided the semi-quantitative chemical composition of burial grounds. The residual gravesoil particles on the bone surface of buried human femurs were removed using a double-sided adhesive tape, mounted on a glass, and coated with graphite in a sputter coater. The backscattered electron (BSE) images of gravesoil particles were performed by a Cambridge Stereoscan 360 microscope, operated at 15 kV accelerating voltage, with a beam size of ~100 nm and a working distance of 11 mm.

3.3 | Bone analyses

3.3.1 | Electron microprobe analysis in wavelength-dispersive mode (EMP-WDS)

EMP-WDS was employed to collect BSE images and perform quantitative chemical analyses on polished thin sections, prepared as reported in Caruso et al. (2018), using a JEOL JXA-8200 EMP-WDS, with an accelerating voltage of 15 kV, a beam current of 5 nA, and counting times of 30 s, on the peak, and 10 s, on the background. BSE images were adopted for a preliminary assessment of the degree of histological preservation of modern and archeological bones, focusing on the biological features (osteons, canaliculi, and osteocyte lacunae) and diagenetic effects (bioerosion and fractures) attributed to the aging test or the effect of the burial environment. Quantitative information about the morphology of biological and

diagenetic pores was extracted by image analysis using the freeware software Fiji (Schindelin et al., 2012), as detailed in Caruso et al. (2021). For quantitative analysis of major (Ca, P) and minor (Fe, Al, Na, K, Si, Mn, Mg, Sr, Ba, S, Cl) elements, natural minerals were used as standards. Raw data were corrected for matrix effects using a conventional ΦρZ routine implemented in the JEOL software package.

3.3.2 | FT-IR

The samples were prepared in KBr pellets following Trueman et al. (2008) for FT-IR spectroscopy. Bone powders were analyzed in transmission mode with a Thermo Scientific™ Nicolet™ iS50 FT-IR Spectrometer equipped with a DTGS detector (spectral range 4000–400 cm^{-1}). The absorption spectra were collected with a spectral resolution of 2 cm^{-1} and recording 64 scans. The reproducibility of the observations was assessed by measuring each sample in duplicate. Instrumental operations, spectra collections, and data analyses were carried out using the Thermo-Nicolet Omnic (version 9) software. For each bone sample, the spectral regions corresponding to characteristic vibrational bands Amide I (1653 cm^{-1}), $v_3(PO_4)$ (1035 cm^{-1}), and $v_2(CO_3)$ (873 cm^{-1}) were studied, as detailed in Caruso et al. (2020). The relative amount of collagen content (Amide I/ PO_4) was obtained by dividing the peak intensity of the Amide I band at 1653 cm^{-1} by the peak intensity of the $v_3(PO_4)$ at 1035 cm^{-1}, and the organic component (wt%) was estimated using the equation of Trueman et al. (2004). The structural carbonate (CO_3/PO_4) was monitored by dividing the intensity band at 873 cm^{-1} of the $v_2(CO_3)$ by the intensity of the phosphate peak at 1035 cm^{-1}. The degree of recrystallization of the bone minerals was determined by the infrared splitting factor (IRSF), calculated by summing the peak intensities of $v_4(PO_4)$ at ~604 and ~590 cm^{-1} and dividing it by the intensity of the valley between them, according to Winer and Bar-Yosef (1990). The mean bone CHA crystallite length was estimated using the equation of Trueman et al. (2008).

4 | RESULTS

4.1 | Gravesoils analysis

Results of the characterization of each gravesoil are reported in Table S1. The particle size distribution evidenced close similarity between both gravesoils, which resulted in rich in silt (~45%) and clay (~36%) fractions and low in sand (15%) and gravel (~5%) fractions. The pH was neutral-basic in G17 (7.38) and increased to an alkaline range in G50 (8.04). The organic carbon content was low in G17 (3.02 g/Kg) and increased in G50 (9.21 g/Kg).

The semi-quantitative analysis by SEM-EDS indicated enrichment in Si, Al, and K of G17 compared with G50, which, conversely, was enriched in Fe, P, and Ca.

The XRD patterns showed the same mineral phases in the gravesoils examined. Quartz resulted as the most abundant phase in G50, followed by calcite and feldspar, whereas plagioclase was predominant in G17. Low amounts of quartz, calcite, and feldspar were also detected in G17. Minor amounts of mica were detected in both samples.

Chemical analysis performed by MP-AES provided a high amount of Ca and Al, followed by Na, P, and Fe in both gravesoils.

4.2 | Chemical analysis of "enriched" solutions

As reported in Table S2, in the solutions used as control the quantities of the major elements did not exceed 50 ppm, with an enrichment in Ca, followed by K, Na, and Mg. The concentrations of trace elements were generally low (~0.02 ppm), except for Sr in S17 (0.74 ppm). Zn, Mn, and Cr were below the detection limit. After 30 days of treatment, SA17_R and SA50_R were rich in Ca (~45 ppm) and Mg (~16 ppm), as shown in Figure 1. A good amount of Na was detected in SA17_C (~57 ppm), whereas Fe resulted below the detection limit.

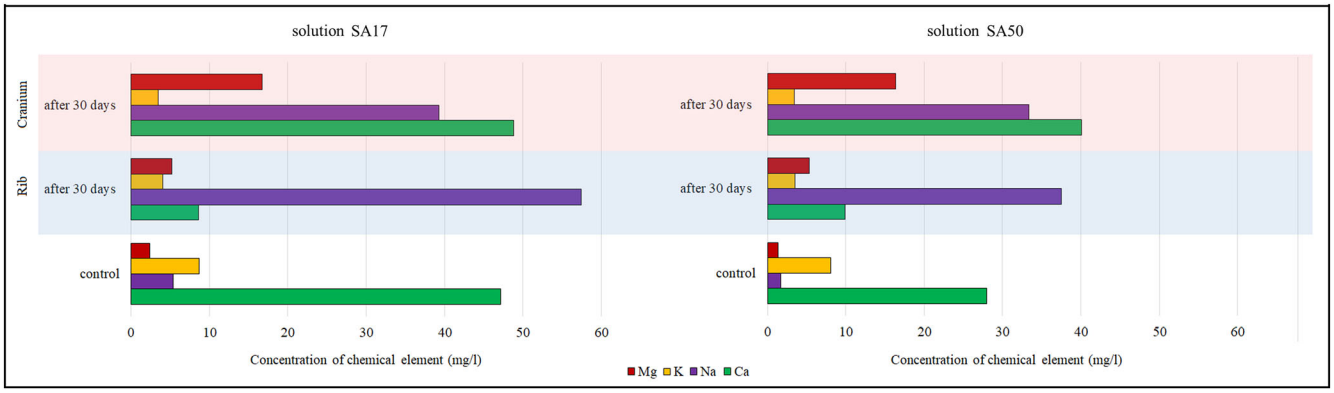

FIGURE 1 Concentrations of the major elements in the solutions analyzed before and after the aging, provided by the MP-AES. [Colour figure can be viewed at wileyonlinelibrary.com]

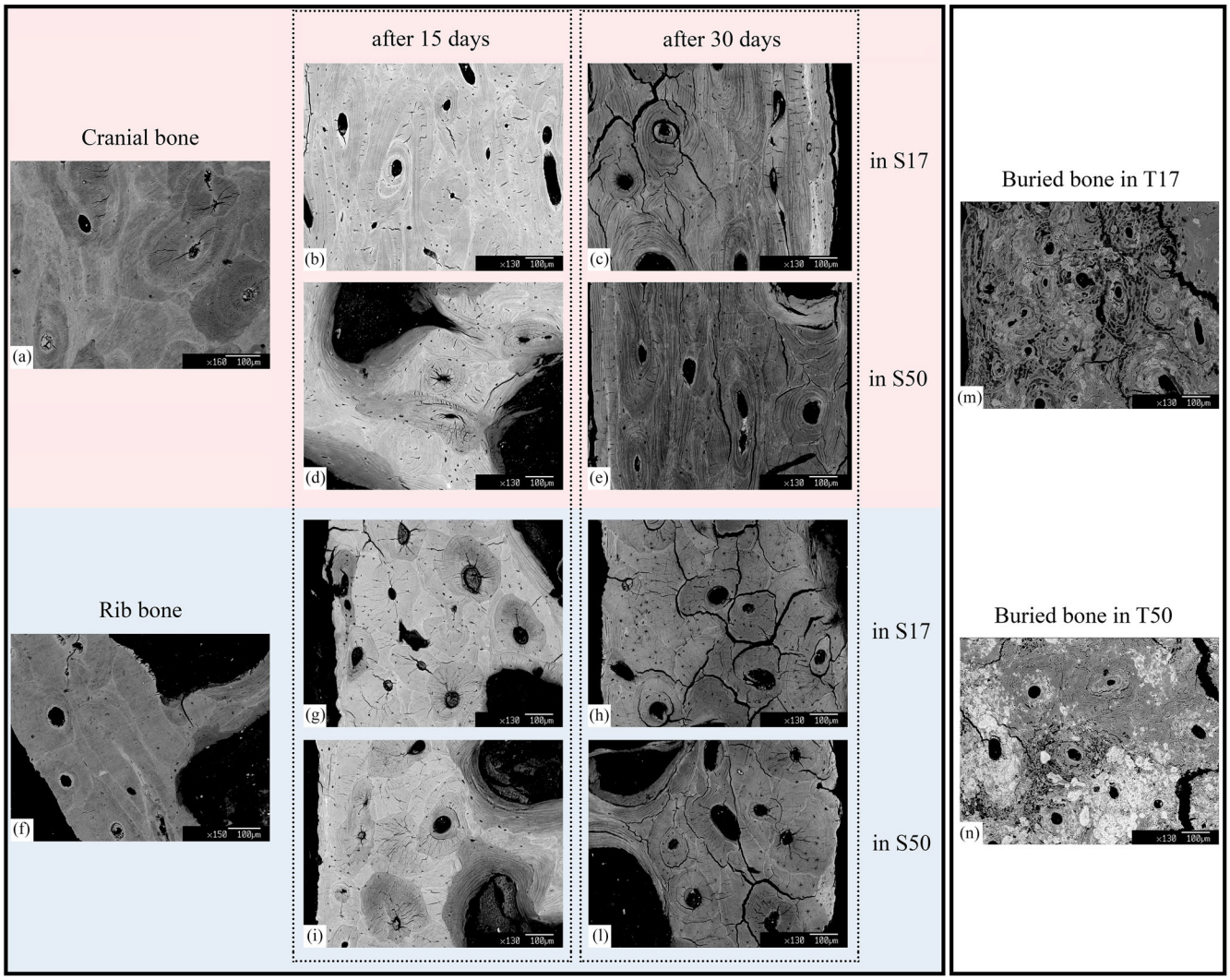

FIGURE 2 Comparison of the cortical bone histology from BSE images provided by EMPA analysis, before and after the aging, compared with buried samples. Control samples for cranium and rib bones are illustrated in (a) and (f). Cranial bone samples after the aging in S17 are illustrated in (b) and (c), after 15 and 30 days of experiment, respectively. Cranial bone samples after the aging in S50 are illustrated in (d) and (e), after 15 and 30 days of experiment, respectively. Rib bone samples after the aging in S17 are illustrated in (g) and (h), after 15 and 30 days of experiment, respectively. Rib bone samples after the aging in S50 are illustrated in (i) and (l), after 15 and 30 days of experiment, respectively. Figures (m) and (n) provide the bone histology of buried samples from T17 and T50, respectively.

4.3 | Bones

4.3.1 | Histological analysis

BSE images of aged bones, reported in Figure 2, evidenced a high degree of histological preservation, compared with buried samples. This included all the main microstructural features isolated employing image analysis tools, such as osteons, canaliculi, and osteocyte lacunae. Significant modifications were detected in the total bone porosity (TBP), since after 15 days, which resulted from histomorphological changes on biological macropores and micropores (highlighted in blue and red in Figure 3, respectively), as well as from diagenetic damages, comprising macrofractures and microfractures (depicted green in Figure 3). As graphically illustrated in Figure 4, TBP was around 3% in the fresh samples, and during the experiment, it remained almost constant in cranial bones (4%), but it increased up to 13% in rib bones. Despite its similar total value, TBP in cranial bones exhibited some evolution. The mean biological macroporosity (i.e., Haversian canals) was not much affected by aging. In contrast, biological microporosity (i.e., lacunae and canaliculi) decreased during the experiment in both burial gravesoil solutions. This decrease was compensated by increased diagenetic porosity, promoted by a widespread diffusion of macrofractures and microfractures. In rib bones aged in S17, the general rise of TBP involved both biological and diagenetic porosity, with the highest percentage of biological macroporosity observed after 15 days (6%) and a decrease after 30 days (3.8%). In rib bones aged in S50, a significant increase of biological macroporosity was observed only after 30 days of the experiment, with a value up to 7.5%. The aging in S17 increased the amount of biological microporosity after 15 days, whereas in S17, it did not affect this type of porosity much.

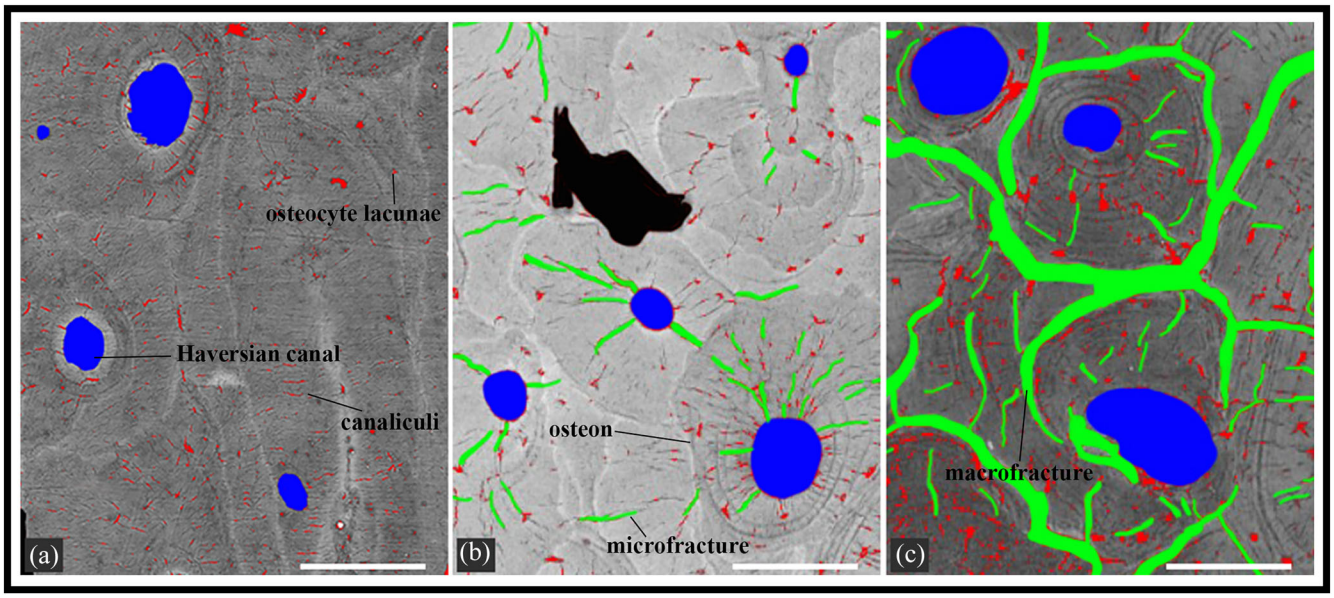

FIGURE 3 BSE images of rib bones taken before (a), after 15 days (b), and 30 days (c) of the aging. With different colors are highlighted: biological macroporosity in blue, biological microporosity in red, and diagenetic fractures in green (scale bar = 100 μm). [Colour figure can be viewed at wileyonlinelibrary.com]

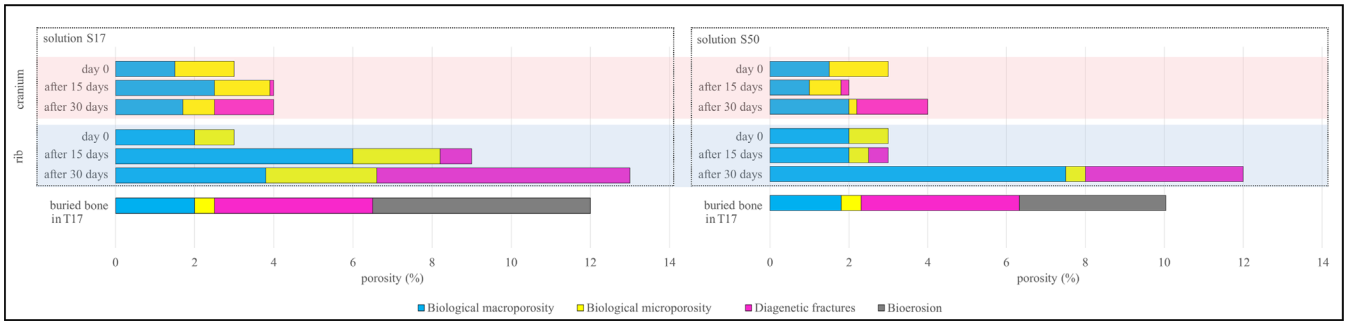

FIGURE 4 Graphical representation of the fractions of biological and diagenetic porosity with respect to the total porosity reported for each aged and buried bone analyzed (e.d.s. 10%). [Colour figure can be viewed at wileyonlinelibrary.com]

Notably, the diagenetic porosity was significantly higher in rib bones (4%–6.4%) compared with cranial bones (1%–1.8%), with a high impact on TBP. The changes in the biological porosity indicated that the accelerated aging process induced modifications of the histological traits at the macroscale and microscale. The quantitative results of histological analysis, reported in detail in Table S3, provided evidence of the enlargement of average vascular canal diameters, due to the erosion of the inner border of Haversian canals in all the aged bones. As graphically illustrated in Figure S1, during aging, the average value of the maximum diameter grew from 40 up to 70 μm; at the same time, the average value of the minimum diameter increased from 30 to 50 μm, leading to a general increase of the calculated mean area of biological macroporosity, from 3000 to 11,000 μm^2. In the same figure, a slight enlargement of osteocyte lacunae during the experiment could also be noticed; the average minimum and maximum diameter increased from 2 to 6 μm and from 3 μm up to 11 μm, respectively. Hence, the calculated mean area of osteocyte lacunae grew from 20 to 160 μm^2 with aging. Moreover, a slight increase in the mean length of bone canaliculi during the experiment (ranging from 20 to 60 μm) was observed, thus increasing the related mean area (from 27 to 90 μm^2).

Both cranial and rib-aged bones appeared seriously fractured. After 15 days of aging, microfractures were widespread within the tissue (Figure 2b,d,g,i), running perpendicularly to the contact between adjacent osteons and/or running radially outward from the Haversian canals. After 30 days of aging, some new microfractures also appeared near the edge of the outer cortical layer, running parallel to it. Microfractures had an average length of 30 μm, an average width of 3 μm, and a related mean area attested around 100 μm^2. Macrofractures were also widespread after the testing (Figure 2e,h,l), and they primarily run around the outer borders of osteons and/or parallel to lamellae bounds. With aging, the average length of macrofractures increased from 80 to 228 μm, keeping an equal width of 6 μm. The

estimated mean area of macrofractures increased from 270 to 2090 μm^2 after 15 and 30 days of testing, respectively.

When the cortical bone tissue of buried bones is considered a widespread alteration of the original microstructure was observed. Figure 2m,n illustrates numerous large and irregular grooves small pores and thin channels (black in color), caused by microorganisms' colonies. These voids are surrounded by brighter micrometric hypermineralized rings originating from the recrystallization of bone apatite due to microbial activity. Numerous microfractures related to bone histology were present within the tissue, together with multidirectional macrofractures, whose morphology and orientation did not follow the original histological traits.

In the buried samples, the TBP ranged from 10% to 12% (Figure 4). Of the original biological porosity, mainly on the outer border of the cortical bone, only Haversian canals could be recognized (1.8%–2%). Indeed, canalicular networks and osteocyte lacunae (0.5%) were poorly preserved and hard to identify, because of the remnants of microbial activity (3.7%–5.5%) and their incorporation in the widespread macrofractures and microfractures (4%). Although histomorphological results provided similar values of biological microporosity between the buried samples, with a mean area of osteocyte lacunae and canaliculi of 38 and 20 μm^2, respectively, biological macropores were enlarged in B17 (mean area of 7500 μm^2) compared with B50 (mean area of 4400 μm^2). The mean area of diagenetic macrofractures was higher in B50 (6300 μm^2), compared with B17 (approximately 2600 μm^2), even if the mean area of diagenetic microfractures appears quite similar in both bones (80 μm^2) (Table S3).

4.3.2 | Organo-mineral and chemical analysis

The collagen preservation, described by the Amide I/PO_4 ratio, decreased from 0.48–0.52 in the fresh samples to 0.40 after 30 days of artificial aging (Figure 5). According to the PO_4 content reported in

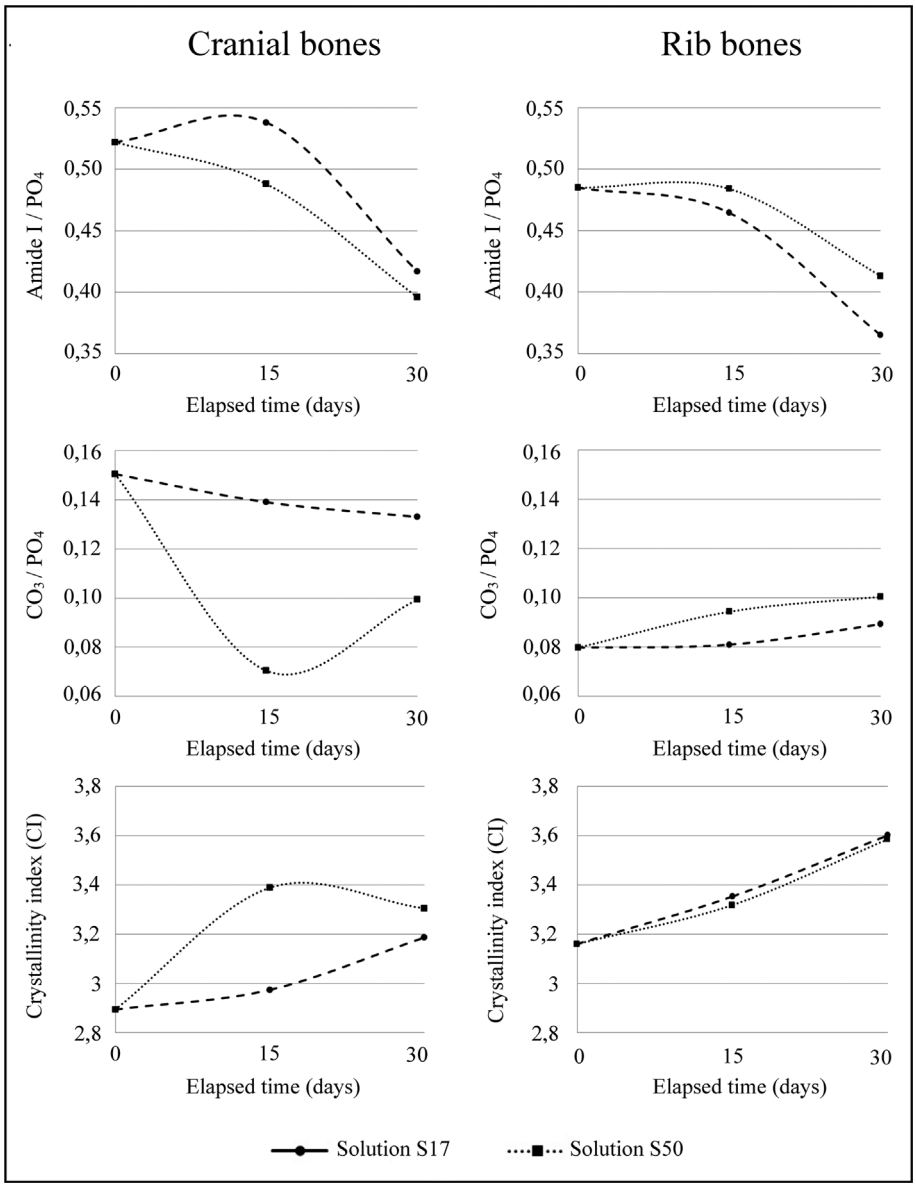

FIGURE 5 FT-IR results provided during the aging test in cranial and rib bones.

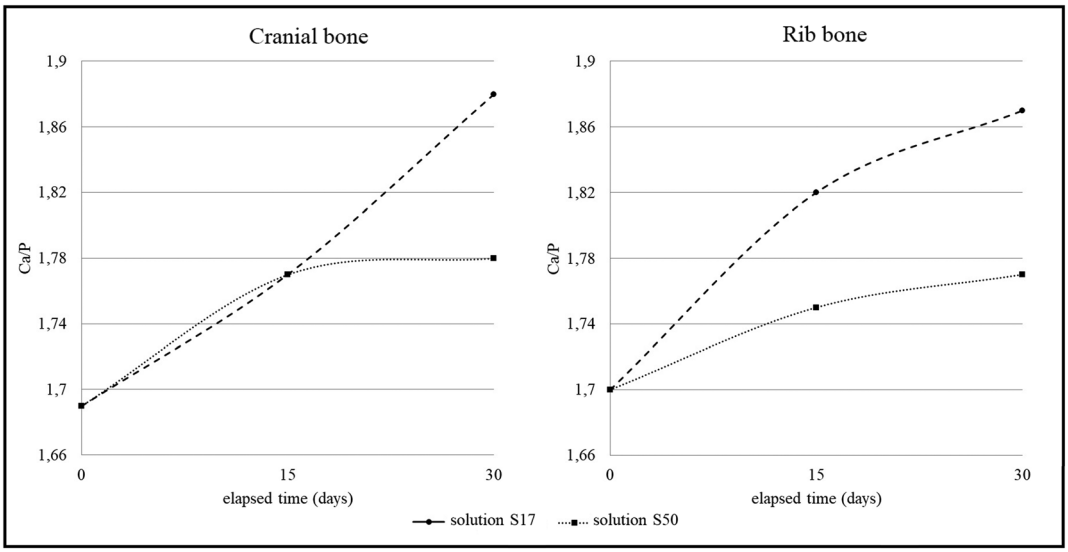

FIGURE 6 Trend of Ca/P ratio observed during the aging test in cranial and rib bones in the two solutions.

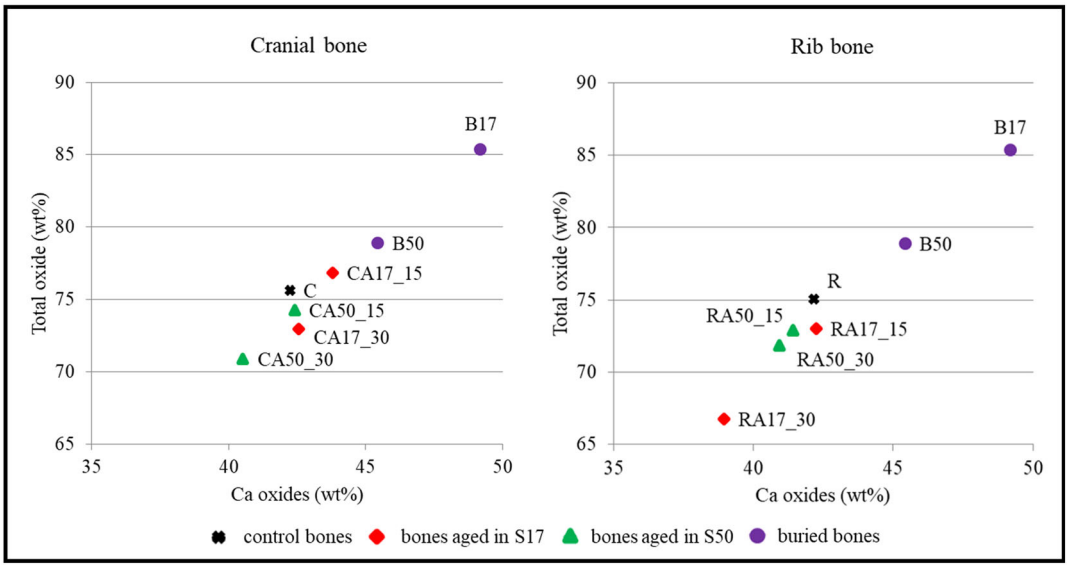

FIGURE 7 Correlation between the Ca content and the total oxide content in cranial and rib bones compared with buried bones. [Colour figure can be viewed at wileyonlinelibrary.com]

Table S4, this is essentially contributed by the decrease in Amide I content. In B17 and B50, the Amide I/PO_4 reached only 0.13, indicating a more substantial loss of the organic fraction over time. Indeed, the weight percentage of the organic fraction was similar in control and aged bones (28–29 wt%), whereas, in buried samples, it was lower (22 wt%) (Table S4).

Results of chemical analysis, presented in Table S5, indicated that in all samples, the carbonated-hydroxyapatite (CHA, $Ca_5(PO_4, CO_3)_3(OH)$) was the only mineral phase within the bone, exhibiting a similar average chemical composition in terms of major oxides.

As illustrated in Figure 6, the Ca/P ratio increased with aging, from ~1.70 in fresh samples to 1.88 after 30 days. This increment proceeded faster in cranial and rib bones aged in S17, compared with the samples aged in S50. Moreover, after 15 days of aging, in S17, the Ca/P ratio resulted higher in rib bones (1.82) compared with cranial bones (1.77).

The Ca/P ratio of B17 and B50 was 1.78, equal to values observed in bones aged for 30 days in S50 (Table S6).

Buried samples provided a higher value of the sum of the total oxide contents (~80 wt%) compared with cranial and rib bones, before and after the aging process (~70 wt%). During the aging, the content of calcium oxides remained low, around 39 wt%, compared with buried specimens, which reached 47 wt% (Figure 7). EMPA analyses also outlined an increase of approximately 10% of the content of the total oxides and of Ca and P oxide in the secondary lamellae with respect to the osteons, both in aged and buried bones. Considering the minor elements (i.e., with concentrations of <1 wt% in oxide),

ionic substitutions of Ca^{2+} and P^{3+} in the mineral structure were detected; Na^{+} and Mg^{2+} in place of Ca^{2+}, as well as substitution of SO_4^{2-} in place of PO_4^{3-}, occurred in all samples. Amounts of SiO_4^{4-} were detected only in bones aged for 30 days. Regarding the ionic substitution of the OH^{-} group, F^{-} resulted below the detection limit, and Cl^{-} was similar in all the bones examined.

The analysis of the vibrational bands of the carbonates and phosphate groups (Figure S2), evidenced that the aging process induced changes in the CO_3/PO_4 ratio, which appeared to depend on the skeletal element considered (Table S4). In cranial bones, the ratio decreased in both solutions during aging (e.g., from 0.15 to 0.10). In S50, the lowest value was reached already after 15 days of testing. Conversely, in rib bones, the CO_3/PO_4 ratio exhibited a slight increase with age, starting from a value lower than the one observed in cranial bone (0.08) (Figure 5). Such values could be considered the same as those detected in the buried bones (0.09).

An inverse relationship has been established between the CO_3/PO_4 ratio and crystallinity index (CI). The CI appears slightly higher in C (3.16), compared with R (2.89), and in both cases, it increased during aging. In cranial bones aged in S17, a faster and higher increase of CI occurred after 15 days of testing (3.39), but after 30 days, similar values were assumed in both solutions (3.30). In rib bones, the CI exhibited a slow linear increase in both solutions (Figure 5), from 3.3 to 3.6, which is the value detected in the buried bones (3.61).

During aging, the mean crystal length (MCL) of bone minerals, calculated based on the IRSF, increased (Table S4). The MCL resulted in 45 and 48 nm in fresh cranial and rib bones, respectively. With aging, it increased to 49 nm in cranial bones and 58 nm in rib bones; the latter value was the same detected in the buried samples (58 nm).

5 | DISCUSSION

The main aim of this study was to test a new laboratory-based method to artificially induce bone diagenesis during a short period (1 month) in fresh human bones. The interaction of the bone material with the burial environment induces microstructural modifications and physical–chemical changes in the bone matrix (Caruso et al., 2020, and references therein). The conditions triggering deterioration act on a long time-scale, over which they are not necessarily constant; hence, in this complex scenario, reproducing the damage patterns is a challenging task. To illustrate this phenomenon, several approaches have been proposed, which cover the entire process of diagenesis in bones, such as the histological preservation, changes in porosity, conservation of carbonate and collagen content, mineral crystallinity, and chemical exchanges (incorporation or release) (Keenan, 2016, and references therein).

5.1 | Bone diagenesis in aged and buried samples

Overall, as illustrated in Figure 8, the differences observed between aged and buried bones primarily concern their microanatomy, whereas the mineral–chemical signature exhibits similar evolution during both artificial and natural aging.

5.1.1 | Histology and porosity

From a histological point of view, the aged bones displayed well-preserved structures (e.g., osteons, vascular canals, and osteocyte lacunae), whereas less than 50% of the original tissue was preserved in buried bones. In addition, voids (~5% of TBP), in the 1–10 μm size range, appeared only in buried bones. This is attributed to the

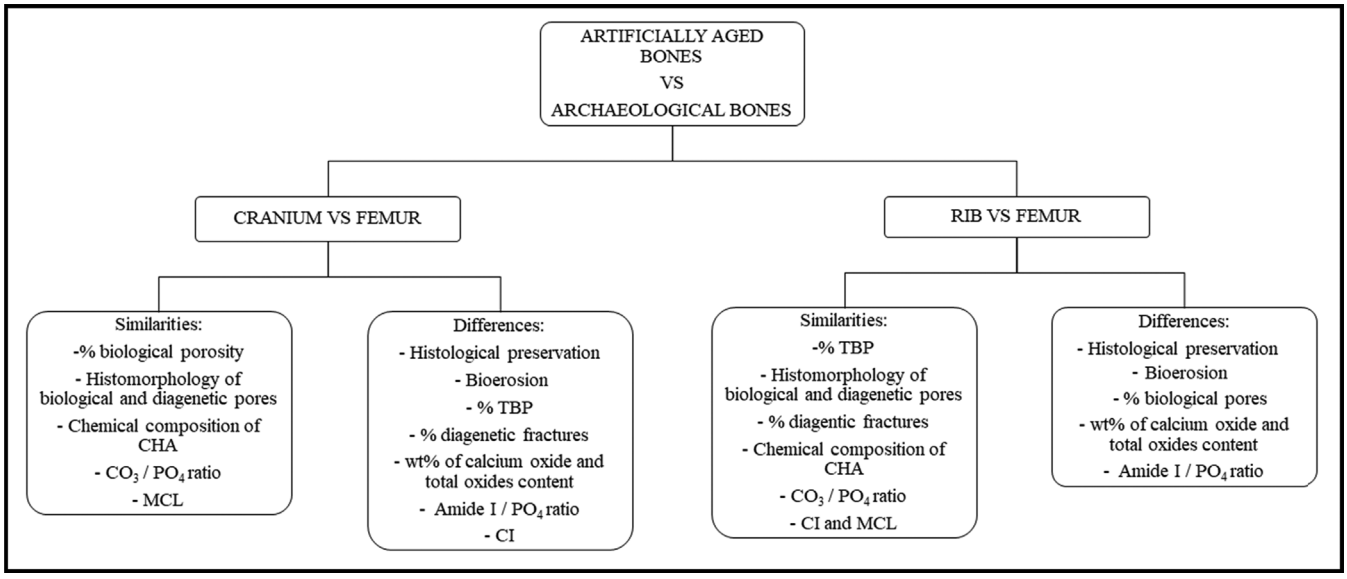

FIGURE 8 Similarities and differences between buried and aged bones at histological scale and in the organo-mineral assessment.

concerted effect of bioerosion by gut-derived and environmental bacterial activity, as well as to the shallow burial depth and periodic waterlogging (Tibbett & Carter, 2008), which likely negatively impacted on bone preservation (Luretta Valley is in the proximity of the Trebbia river). Indeed, only in buried bones were we able to detect the typical effect of the biogenic degrading microorganisms (the so-called bioerosion or microorganisms boring; Hackett, 1981). This osteolytic activity creates typical porosities, as a result of swelling of collagen fibers, solubilization, leaching, and redistribution of carbonate-hydroxyapatite (Child, 1995; Hedges et al., 1995). The absence of bioerosion effects in aged bones might be ascribed to several factors, such as (i) the removal of soft tissues on fresh bones (Delannoy et al., 2018; Hollund et al., 2012; Smith et al., 2007; Trueman & Martill, 2002); (ii) the use of gravesoil solutions resulting by the leaching of burial soils in distilled water, pre-treated with hydrogen peroxide to destroy the organic matter (and possible microorganisms); (iii) the absence of bacterial inoculation to simulate the biogenic degradation in soil (Delannoy et al., 2018); and (iv) the high temperature employed to accelerate the bone degradation kinetic (High et al., 2015). Although the microorganisms' involvement is crucial in the diagenetic process, the use of sterile enriched solutions should be invoked to justify the well-preserved organic fraction in aged bones. This aspect should be considered in the experimental design for future research.

Diagenetic porosity is common both in aged and buried bones and comprises two types of diagenetic fractures: (i) microfractures promoted by the general reorganization of the organo/mineral and chemical components of bones, following the collagen leaching (Delannoy et al., 2018; Pfretzschner, 2004). Fluctuation in moisture, temperature, and water of the surrounding environment in burials, as well as sample storage practices (Karr & Outram, 2015), alter the collagen structure and bone chemistry, generating microfractures due to expansion and contraction of the tissue (Pfretzschner & Tütken, 2011); (ii) macrofractures, which do not follow the morphology of the histological bone structures, are either originated from physical stress in burials (such as mechanical pressures, animal scavenging, anthropological activities, and so forth) or they form during sample preparation (Dal Sasso et al., 2014; Lander et al., 2014; Tripp et al., 2018; Turner-Walker, 2012), without necessarily leading to or resulting from collagen degradation (Tripp et al., 2018, and references therein). Again, the high temperature used in the experiment could have impaired the fracture toughness and weakened the hydrogen bonding between collagen fibrils (Yan et al., 2007).

Figure 4 clearly illustrates that macroporosity and microporosity evolved differently during aging. In cranial bones, the percentage of biological macropores was similar to that observed in buried bones (approximately 2%), whereas in rib bones, it increased to approximately 8% after aging. At the same time, the percentage of biological micropores dropped to 0.5% during the experiment, the same value of buried bones, with the exception of the rib bones aged in S17, whose microporosity value increased to approximately 3%. This macroporosity-increasing and microporosity-decreasing in percentage can be attributed to the bone matrix's protein loss and mineral dissolution, confirming the results of Nielsen-Marsh and Hedges (2000). It must be noted that the authors evaluated only the nominal radius of pores (starting from 4 nm) with no distinction between biological and diagenetic pores. Moreover, macroporosity and microporosity were distinguished according to the results of mercury intrusion porosimetry. In the current study, the sub-micron pores (less than 0.1 μm in diameter) were not accessible because of the resolution of the BSE-SEM. In addition, in our case, the method adopted to detect the porosity suffered from some limitations. First of all, a single transverse cross-section may not represent the whole sample (Mandl et al., 2022, and references therein). Moreover, some inaccuracy may originate during the image processing step aimed at separating pores from the bone matrix, especially for the finer porosity. Therefore, even if the correlation between macroporosity and microporosity has been established, the data are not directly comparable, and only further investigation could clarify this diagenetic effect.

5.1.2 | Organo-mineral and chemical assessment

Despite the high discrepancy in the conservation of the bone microanatomy, both aged and buried bones preserved a high amount of collagen. Indeed, the measurement of the absorption intensity band of ν_1Amide I (1653 cm^{-1}) evidenced an alteration of the organic fraction only in buried bones, as evidenced by the relative amount of collagen (Table S4). It is reasonable to suppose that the temperature adopted during the experiment was not high enough to induce a significant loss of the organic component (High et al., 2015). Indeed, the mineralized collagen is not readily susceptible to collagenase degradation, requiring relatively high temperature for denaturation (over 50°C) (Child, 1995; Collins et al., 2002; Hedges et al., 1995). In addition, the absence of microbes contributed to the preservation of collagen structures. This is confirmed by the observation that bones undergoing defleshing, butchering, or rapid skeletonization processes are often free of bioerosion, because of the limited degree of putrefactive decomposition and the related microbial damage (Hollund et al., 2012). Anyway, the neutral-mild alkaline pH of the burial environment might have inhibited the chemical hydrolysis of collagen (Collins et al., 2002), being favored by pore-water fluctuations and extreme pH values (Delannoy et al., 2018; High et al., 2015; Nielsen-Marsh & Hedges, 2000). However, it must be noted that, during burial, the degree of collagen preservation is extremely heterogeneous (Caruso et al., 2018, 2020), since it depends both on the environmental settings (i.e., pH, temperature, humidity, and soil composition) and on in vivo bone structures (Caruso et al., 2018, 2020, 2021; Collins et al., 2002; Gatti et al., 2022; Hollund et al., 2013; Keenan et al., 2015; Lebon et al., 2011, 2016; Nielsen-Marsh et al., 2000; Nielsen-Marsh & Hedges, 2000; Reiche et al., 2010; Trueman & Martill, 2002; Turner-Walker, 2012; Viani et al., 2021).

Since the mineral and organic phases are tightly intergrown and mutually protect each other, because of the intimate association of apatite crystals and collagen fibrils at the nanoscale, every change in

the organic matrix potentially affects the preservation of the mineral fraction.

All the indicators pointed to well-preserved mineral fraction in all the bones studied. Moreover, the uptake of exogenous elements (from soil [Bayari et al., 2020; López-Costas et al., 2016; Rogoz et al., 2012] and/or decomposition [Collins et al., 2002; Krajcarz, 2019]) into the original CHA crystals was limited, both in aged and buried samples. This might be due to the neutral-mild alkaline pH of the experimental setting and of the burial environment.

The aging experiment increased the calcium-to-phosphate molar ratio only in bones immersed in S17, since they share the same ratio of buried bones (1.78). On the contrary, the chemistry of S50 could not induce significant changes in the bone bioapatite, since the Ca/P value remained relatively constant.

Considering the ionic substitutions mediated by physiological processes in vivo (Keenan et al., 2015; Margariti et al., 2019), only the weight percentage of Na (in place of Ca in CHA crystal sites) significantly decreased during the experiment, reaching the same value of buried bones after 30 days. Indeed, because of its high solubility and low sorptivity, sodium is readily leached out from bones after burial (Reiche et al., 2002). Contrarily, even if the buried bones provided a low level of manganese, the induced degradation process did not alter the content of this chemical element in aged bones.

Overall, the sum of the total oxide content into the CHA remained low in all aged bones, since the amount of organic carbon, lipids, and water was well preserved.

The presence of carbonate into the bioapatite makes the mineral structure relatively unstable and disordered, hence a general reorganization/growth of carbonated-hydroxyapatite crystals, to reach a more thermodynamic stable form (increased crystals size, lattice perfection, and reduced specific surface area; Trueman et al., 2004), is widely attested after death; the diagenetic conditions of burial trigger the process (Kontopoulos et al., 2019). During the aging experiments, FT-IR spectra evidenced slight changes in the carbonate absorption band (at 873 cm^{-1} [v_2]). Such changes were influenced by both the type of bones and the gravesoil solutions (see details below). Nonetheless, at the end of the experiments, aged and buried bones shared the same CO_3/PO_4 (0.09).

During aging, in cranial bones, as the CO_3/PO_4 ratio decreased, the calculated crystallinity index increased, whereas in rib bones, both parameters increased. Moreover, in aged rib samples, the crystallinity value was similar to the one of buried bones (3.6), whereas in the cranium, it remained lower (3.2). As a consequence, after the experiment, MCL in rib-aged bones was higher (58 nm) and more similar to one of the buried samples, compared with the cranium (50 nm). The general increase in IRSF values indicates an amelioration of the mineral crystallinity, as a result of crystal re-organization and/or growth of bioapatite (Nielsen-Marsh & Hedges, 2000; Trueman, 2013).

These results indicate that aging induced significant changes in bone porosity and minero-chemical fraction. Both natural and artificially induced diagenesis acted on (i) the degradation of the biological porosity and the propagation of diagenetic fractures; (ii) the preservation of the bioapatite and its chemical exchange and substitution; and (iii) the alteration of the carbonate and mineral crystallinity.

Even if this thermal condition is not comparable with one developed during the diagenesis in the natural soil, it allows reaction rates higher than those expected at room temperature, making the study of bone degradation possible at laboratory time scale.

5.2 | Influence of the type of bone on the artificial aging in the two solutions

Although the cranium and the rib were aged under the same conditions, some diagenetic features changed differently, as illustrated in Figure 9, according to the type of bone (i.e., biological porosity, post-mortem fractures, CO_3/PO_4, and IRSF) and the chemistry of the solution (i.e., Ca/P and CO_3/PO_4).

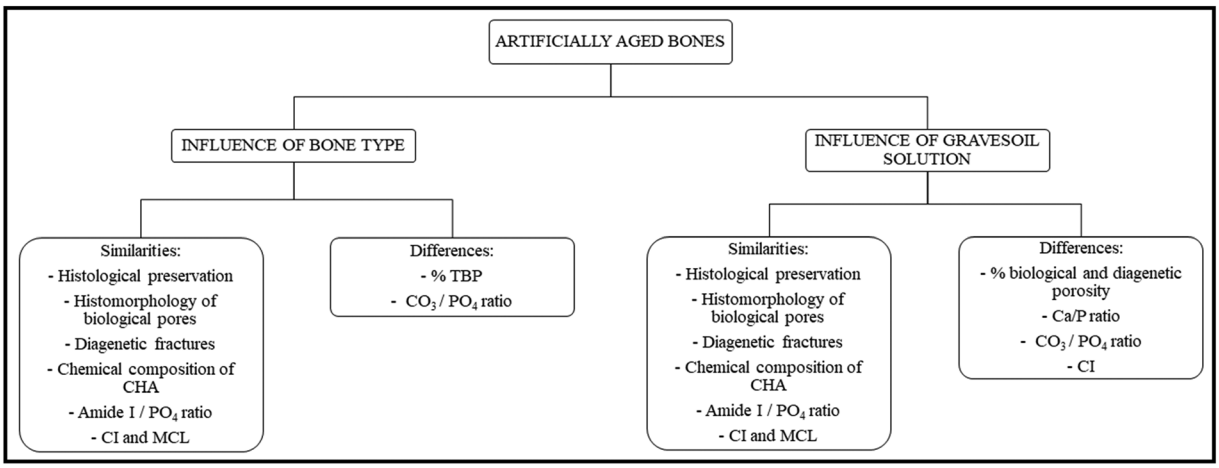

FIGURE 9 Summary of the similarities and differences observed in bones after aging influenced by the type of bone and the 'enriched' solution employed.

Regarding the bone histology, after the experiment a larger propagation of diagenetic fractures and a higher enlargement of natural pores were observed in the rib, leading to a higher increase of the TBP (12%) compared with the cranium (4%). Cranial and rib bones differ in the orientation of the osteons and their related structures, being subjected to different biomechanical stresses (Cormier et al., 2003); this made the rib more easily subjected to diagenesis. Hence, according to the type of bone tissue, the porosity tends to follow a particular degradation path, even in the same site-environmental context (Caruso et al., 2020, 2021; Dal Sasso et al., 2014; Fernández-Jalvo et al., 2010; Hedges et al., 1995; Jackes et al., 2001; Nielsen-Marsh et al., 2000; Nielsen-Marsh & Hedges, 2000; Reiche et al., 2002; Rogoz et al., 2012; Smith et al., 2002; Trueman & Martill, 2002; Turner-Walker, 2012; Turner-Walker et al., 2002).

When bone chemistry is considered, a general opposite tendency to absorb or release calcium from and into solutions was attested in the cranium and the rib, respectively. Moreover, carbonate from the bioapatite was leached preferentially from cranial bones, compared with ribs, which, on the contrary, exhibited a higher IRSF after the testing. Despite these differences related to the skeletal element, the presence of calcite in S50 influenced the weight percentage of phosphate (increases), and the related Ca/P molar ratio (decreases), in all bones, since this favored dissolution (release of calcium and carbonate) and precipitation processes (uptake of phosphate) (Ren et al., 2021) in the same manner. In the cranium, the loss of the structural carbonate induced both the dissolution of the most unstable phases of the original CHA (Nielsen-Marsh & Hedges, 2000) and the precipitation of a new more stable (secondary) hydroxyapatite (Caruso et al., 2020; Trueman et al., 2004, and references therein). In ribs, the high preservation of biogenic carbonate and the absence of any diagenetic CO_2^{3-} incorporation into the bioapatite lattice allow us to hypothesize a general re-arrangement of the original mineral phase toward a more stable form, without chemical exchange with the gravesoil solutions, even in calcitic environment (Monasterio-Guillot et al., 2022; Nielsen-Marsh & Hedges, 2000).

5.3 | Limitations of the study

In this study, preliminary results of a new approach to replicate bone modifications induced by natural diagenesis are presented. Although some damage patterns have been successfully reproduced at the laboratory scale during a very short period (30 days), some issues need to be considered. They include the use of temperature to accelerate the bone degradation processes, which, although previously adopted (High et al., 2015), may have diverted the diagenetic path away from the natural one, as discussed in Section 5. Therefore, further work is needed to clarify this aspect. Moreover, as mentioned above, the role of microbial activity in the grave soils has been excluded by sterilizing the solutions. Given the importance of this biological agent of bone diagenesis, it must be considered in the experimental design for future research. Future work must also include (i) a higher number of samples; (ii) more skeletal elements; (iii) consistent types of bones for comparison between archaeological and artificially aged ones; (iv) a broad range of biological ages (i.e. children), female individual, and different ethnicities; and (v) other burial environments.

6 | CONCLUSIONS AND FUTURE DIRECTIONS

This study was mainly aimed at providing a new laboratory-based method to replicate the bone deterioration effects caused by the burial environment (specifically, the burial soil) observed in the ancient osteological material. Degrading experiments are common to understand and predict the long-term behavior of skeletal materials, mainly to gain information regarding the decay rates of bones. In this light, the present research highlights:

i. The most significant variation between aged and buried bones mainly involved the bone microstructure. Indeed, because of the sample preparation and experimental setting, the lack of bacteria in aged samples inhibited the typical development of biogenic degrading microorganisms, which was well represented in the buried skeletons, leading to a higher value of diagenetic porosity.
ii. Despite the different paths, the remaining biological pores and the post-mortem fractures evolved with the same histomorphology during the artificial and natural diagenesis. The natural assessment of bone itself seems to have partially influenced the evolution of the porosity during the test, since its percentage remains high in rib bones during the whole experiment, rather than in cranial bones (where the values are generally lower), irrespective of the chemistry of the "enriched" solutions.
iii. As for the chemical-mineralogical aspects, the carbonate-hydroxyapatite remained the primary phase in aged and buried bones, with few ionic substitutions derived from the surrounding environment or putrefactive processes. Overall, a low carbonate level and a high crystallinity index (and consequently mineral crystal length) were provided both after the aging and in the buried samples, being these parameters more strictly related to the proceeding of the diagenesis. The composition of bioapatite was influenced by the chemistry of the "enriched" solutions more than the other parameters considered. Indeed, the Ca/P molar ratio increases more in bones immersed in S50, irrespective of the type of bones employed, reaching the same values of buried bone. On the contrary in the bones immersed in S17, the Ca/P molar ratio remains low, and the increase from control bones is minimal.
iv. Despite this similar chemical-mineral assessment of the bone bioapatite, a higher lipid, water, and organic carbon content was still present only in aged bones. Similarly, the organic content remained high during aging, whereas it decreased in buried bones because of the digestion of collagen proteins by microbes.
v. Compared with previous experiments, the present method appears fast, inexpensive, and reproducible and gives easier accessibility and more availability to the bone materials.

Moreover, the accelerated aging requires minimal sample preparation, is not too time consuming, and can be performed only at the laboratory scale.

In conclusion, the results are thought to contribute to the knowledge of how the microstructural modifications and physical–chemical properties of the bone materials interact with the burial environment and how possible to re-create and study the diagenetic changes induced in natural soil at the laboratory scale. A more significant number of samples and the use of different types of bones and soil will improve these preliminary results to bring more understanding of the diagenesis of human remains in various types of soil and burial conditions, having this research an extensive applicability both in the forensic and the archaeological field, that is, to reconstruct and track the burial environment and to investigate to which taphonomic process the bone underwent.

AUTHOR CONTRIBUTIONS

Caruso Valentina, Viani Alberto, and Marinoni Nicoletta wrote the main manuscript text. Caruso Valentina, Marinoni Nicoletta, and Diella Valeria performed EMP analysis on bones and interpreted the results. Caruso Valentina and Possenti Elena performed FT-IR analysis on bones and elaborated the data. Caruso Valentina and Ferrari Elena performed MP-AES analysis on the solution of gravesoils and on "enriched" solutions and elaborated the data. Caruso Valentina and Trombino Luca performed chemical and SEM-EDS analysis of gravesoils and interpreted the results. Caruso Valentina and Cattaneo Cristina collected the fresh bone materials, performed histological analysis, and interpreted the data. All authors assisted in data interpretation and revision of the manuscript.

ACKNOWLEDGMENTS

The authors would like to thank Dr. Roberta Conversi of Soprintendenza per i Beni Architettoni e Paesaggistici di Parma e Piacenza and Dr. Maria Maffi of Museo Civico di Travo to have provided the archeological materials and supported the research with their depth knowledge of the territory and the historical period. The authors would also like to thank the staff of LABANOF, Laboratorio di Antropologia e Odontologia Forense, of Università degli Studi di Milano (Milan, Italy), for their support in collecting, storing, and studying the fresh osteological materials, and the staff of EMP and XRD laboratories of Università degli studi di Milano, Dipartimento di Scienze della Terra "Ardio Desio" (Milan, Italy), for their precious technical support for data collection.

CONFLICT OF INTEREST STATEMENT

The authors declare that they have no conflict of interest.

DATA AVAILABILITY STATEMENT

The data that supports the findings of this study are available in the supplementary material of this article

ORCID

Valentina Caruso https://orcid.org/0000-0001-9452-9121

REFERENCES

Avery, B.W. (1974). Soil survey, technical monograph no. 6: Soil survey laboratory methods. Harpenden.

Bayari, S. H., Özdemir, K., Sen, E. H., Araujo-Andrade, C., & Erdal, Y. S. (2020). Application of ATR-FTIR spectroscopy and chemometrics for the discrimination of human bone remains from different archaeological sites in Turkey. *Spectrochimica Acta Part A: Molecular and Biomolecular Spectroscopy*, *237*, 118311. https://doi.org/10.1016/j.saa.2020.118311

Behrensmeyer, A. K. (1978). Taphonomic and ecologic information from bone weathering. *Paleobiology*, *4*(2), 150–162. https://www.jstor.org/stable/2400283

Berna, F., Matthews, A., & Weiner, S. (2004). Solubilities of bone mineral from archaeological sites: The recrystallization window. *Journal of Archaeological Science*, *31*, 867–882. https://doi.org/10.1016/j.jas.2003.12.003

Boaks, A., Siwek, D., & Mortazavi, F. (2014). The temporal degradation of bone collagen: A histochemical approach. *Forensic Science International*, *240*, 104–110. https://doi.org/10.1016/j.forsciint.2014.04.008

Brooks, S., & Suchey, J. M. (1990). Skeletal age determination based on the os pubis: A comparison of the Acsádi-Nemeskéri and Suchey-Brooks methods. *Human Evolution*, *5*, 227–238. https://doi.org/10.1007/BF02437238

Buikstra, J.E. & Ubelaker, D. (1994). Standards for data collection from human skeletal remains. Arkansas archeological survey. *Research series*, 44. Fayetteville. https://doi.org/10.1002/ajhb.1310070519

Caruso, V. (2017). Degradation of organic and mineral phases in buried human remains: The Earth Sciences analytical characterization. Ph.D. thesis, Università degli Studi di Milano.

Caruso, V., Cummaudo, M., Maderna, E., Cappella, A., Caudullo, G., Scarpulla, V., & Cattaneo, C. (2018). A comparative analysis of microscopic alterations in modern and ancient undecalcified and decalcified dry bones. *American Journal of Physical Anthropology*, *165*, 363–369. https://doi.org/10.1002/ajpa.23348

Caruso, V., Marinoni, N., Diella, V., Berna, F., Cantaluppi, M., Mancini, L., Trombino, L., Cattaneo, C., Pastero, L., & Pavese, A. (2020). Bone diagenesis in archaeological and contemporary human remains: An investigation of bone 3D microstructure and minero-chemical assessment. *Archaeological and Anthropological Sciences*, *12*, 162. https://doi.org/10.1007/s12520-020-01090-6

Caruso, V., Marinoni, N., Diella, V., Possenti, E., Mancini, L., Cantaluppi, M., Berna, F., Cattaneo, C., & Pavese, A. (2021). Diagenesis of juvenile skeletal remains: A multimodal and multiscale approach to examine the post-mortem decay of children's bones. *Journal of Archaeological Science*, *135*, 105477. https://doi.org/10.1016/j.jas.2021.105477

Child, A. M. (1995). Towards and understanding of the microbial decomposition of archaeological bone in the burial environment. *Journal of Archaeological Science*, *22*(2), 165–174. https://doi.org/10.1006/jasc.1995.0018

Collins, M. J., Nielsen-Marsh, C. M., Hiller, J., Smith, C. I., Roberts, J. P., Prigodich, R. V., Wess, T. J., Csapò, J., Millard, A. R., & Turner-Walker, G. (2002). The survival of organic matter in bone: A review. *Archaeometry*, *44*(3), 383–394. https://doi.org/10.1111/1475-4754.t01-1-00071

Conversi, R., & Mezzadri, C. (2011). Testimonianze funerarie d'età longobarda nel Piacentino e studio preliminare della necropoli di Sant' Andrea di Travo (PC). In Possenti. (Ed.), *Necropoli Longobarde in Italia. Indirizzi della ricerca e nuovi dati. Atti del convegno internazionale* (pp. 214–244). Castello del Buonconsiglio.

Cormier, J.M., Stitzel, J.D., Duma, S.M., & Matsuoka, F. (2003). Microstructural analysis of osteon orientation in human rib cortical bone.

Proceedings of the 31st international workshop on human subjects for biomechanical research, San Diego (CA).

Crowder, C., & Stout, S. (2011). *Bone histology: An anthropological perspective*. CRC Press. https://doi.org/10.1201/b11393

Dal Sasso, G., Maritan, L., Usai, D., Angelini, I., & Artioli, G. (2014). Bone diagenesis at the micro-scale: Bone alteration patterns during multiple burial phases at Al Khiday (Khartoum, Sudan) between the Early Holocene and the II century AD. *Palaeogeography Palaeoclimatology Palaeoecology*, *416*, 30–42. https://doi.org/10.1016/j.palaeo.2014.06.034

Delannoy, Y., Colard, T., Cannet, C., Mesli, V., Hédouin, V., Penel, G., & Ludes, B. (2018). Characterization of bone diagenesis by histology in forensic contexts: A human taphonomic study. *International Journal of Legal Medicine*, *132*, 219–227. https://doi.org/10.1007/s00414-017-1699-y

Delannoy, Y., Colard, T., Le Garff, E., Mesli, V., Aubernon, C., Penel, G., Hedouin, V., & Gosset, D. (2016). Effects of the environment on bone mass: A human taphonomic study. *Legal Medicine*, *20*, 61–67. https://doi.org/10.1016/j.legalmed.2016.04.006

Fernández-Jalvo, Y., Andrews, P., Pesquero, D., Smith, C., Marín-Monfort, D., Sánchez, B., Geigl, E.-M., & Alonso, A. (2010). Early bone diagenesis in temperate environments Part I: Surface features and histology. *Palaeogeography Palaeoclimatology Palaeoecology*, *288*, 62–81. https://doi.org/10.1016/j.palaeo.2009.12.016

Fisk, S., Berna, F., Merrett, D. C., & Cardoso, H. (2019). Post-mortem gross composition changes and differential weathering of immature and mature bone in an experimental burial environment. *Journal of Archaeological Science: Reports*, *26*, 101904. https://doi.org/10.1016/j.jasrep.2019.101904

Gale, S. J., & Hoare, P. G. (1991). *Quaternary sediments*. Belhaven Press.

Gatti, L., Lugli, F., Sciutto, G., Zangheri, M., Prati, S., Mirasoli, M., Silvestrini, S., Benazzi, S., Tütken, T., Douka, K., Collina, C., Boschin, F., Romandini, M., Iacumin, P., Guardigli, M., Roda, A., & Mazzeo, R. (2022). Combining elemental and immunochemical analyses to characterize diagenetic alteration patterns in ancient skeletal remains. *Scientific Reports*, *12*, 5112. https://doi.org/10.1038/s41598-022-08979-3

Gaudino, S., Galas, C., Belli, M., Barbizzi, S., de Zorzi, P., Jaćimović, R., Jeran, Z., Pati, A., & Sansone, U. (2007). The role of different soil sample digestion methods on trace elements analysis: A comparison of ICP-MS and INAA measurement results. *Accreditation and Quality Assurance*, *12*(2), 84–93. https://doi.org/10.1007/s00769-006-0238-1

Guarino, F. M., Angelini, F., Vollono, C., & Orefice, C. (2006). Bone preservation in human remains from the Terme del Sarno at Pompeii using light microscopy and scanning electron microscopy. *Journal of Archeological Science*, *33*(4), 513–520. https://doi.org/10.1016/j.jas.2005.09.010

Hackett, C. J. (1981). Microscopical focal destruction (tunnels) in exhumed human bones. *Medicine, Science, and the Law*, *21*(4), 243–265. https://doi.org/10.1177/002580248102100403

Hedges, R. E. M. (2002). Bone diagenesis: An overview of processes. *Archaeometry*, *44*, 319–328. https://doi.org/10.1111/1475-4754.00064

Hedges, R. E. M., Millard, A. P., & Pike, A. W. G. (1995). Measurements and relationships of diagenetic alteration of bone from three archaeological sites. *Journal of Archeological Science*, *22*, 201–209. https://doi.org/10.1006/jasc.1995.0022

High, K., Milner, N., Panter, I., & Penkman, K. E. H. (2015). Apatite for destruction: Investigating bone degradation due to high acidity at Star Carr. *Journal of Archeological Science*, *59*, 159–168. https://doi.org/10.1016/j.jas.2015.04.001

Hollund, H. I., Aariese, F., Fernandes, R., Jans, M. M. E., & Kars, K. (2013). Testing an alternative high-throughput tool for investigating bone diagenesis: FTIR in attenuated total reflection (ATR) mode. *Archaeometry*, *55*(3), 507–532. https://doi.org/10.1111/j.1475-4754.2012.00695.x

Hollund, H. I., Jans, M. M., Collins, M. J., Kars, H., Joosten, I., & Kars, S. M. (2012). What happened here?: Bone histology as a tool in decoding the postmortem histories of archaeological bone from Castricum, The Netherlands. *International Journal of Osteoarchaeology*, *22*, 537–548. https://doi.org/10.1002/oa.1273

Jackes, M., Sherburne, R., Lubell, D., Barker, C., & Wayman, M. (2001). Destruction of microstructure in archaeological bone: A case study from Portugal. *International Journal of Osteoarchaeology*, *11*, 415–432. https://doi.org/10.1002/oa.583

Karr, L. P., & Outram, A. K. (2015). Bone degradation and environment: Understanding, assessing and conducting archaeological experiments using modern animal bones. *International Journal of Osteoarchaeology*, *25*, 201–212. https://doi.org/10.1002/oa.2275

Keenan, S. W. (2016). From bone to fossil: A review of the diagenesis of bioapatite. *American Mineralogist*, *101*(9), 1943–1951. https://doi.org/10.2138/am-2016-5737

Keenan, S. W., Engel, A. S., Roy, A., & Bovenkamp-Langlois, G. L. (2015). Evaluating the consequences of diagenesis and fossilization on bioapatite lattice structure and composition. *Chemical Geology*, *413*, 18–27. https://doi.org/10.1016/j.chemgeo.2015.08.005

Kendall, C., Høier Eriksen, A. M., Kontopoulos, I., Collins, M. J., & Turner-Walker, G. (2018). Diagenesis of archaeological bone and tooth. *Palaeogeography Palaeoclimatology Palaeoecology*, *491*, 21–37. https://doi.org/10.1016/j.palaeo.2017.11.041

Kontopoulos, I., Nystrom, P., & White, L. (2016). Experimental taphonomy: Post-mortem microstructural modifications in Sus scrofa domesticus bone. *Forensic Science International*, *266*, 320–328. https://doi.org/10.1016/j.forsciint.2016.06.024

Kontopoulos, I., Penkman, K., McAllister, G. D., Lynnerup, N., Damgaard, P. B., Hansen, H. B., Allentoft, M. E., & Collins, M. J. (2019). Petrous bone diagenesis: A multi-analytical approach. *Palaeogeography Palaeoclimatology Palaeoecology*, *518*, 143–154. https://doi.org/10.1016/j.palaeo.2019.01.005

Krajcarz, M. T. (2019). Alteration of the metal content in animal bones after 2.5-year experimental exposure to sediments. *Archaeological and Anthropological Sciences*, *11*, 361–372. https://doi.org/10.1007/s12520-017-0533-2

Lander, S. L., Brits, D., & Hosie, M. (2014). The effects of freezing, boiling and degreasing on the microstructure of bone. *Homo*, *65*(2), 131–142. https://doi.org/10.1016/j.jchb.2013.09.006

Lebon, M., Müller, K., Bahain, J., Fröhlich, F., Falguères, C., Bertrand, L., Sandt, C., & Reiche, I. (2011). Imaging fossil bone alterations at the microscale by SR-FTIP microspectroscopy. *Journal of Analytical Atomic Spectrometry*, *26*, 922–929. https://doi.org/10.1039/C0JA00250J

Lebon, M., Reiche, I., Gallet, X., Bellot-Gurlet, L., & Zazzo, A. (2016). Rapid quantification of bone collagen content by ATR-FTIR spectroscopy. *Radiocarbon*, *58*, 131–145. https://doi.org/10.1017/RDC.2015.11

López-Costas, O., Lantes-Suárez, O., & Martínez Cortizas, A. (2016). Chemical compositional changes in archaeological human bones due to diagenesis: Type of bone vs soil environment. *Journal of Archaeological Science*, *67*, 43–51. https://doi.org/10.1016/j.jas.2016.02.001

Mandl, K., Duffett Carlson, K. S., Brönnimann, D., McCall, A., Grassberger, M., Teschler-Nicola, M., Weiss-Krejci, E., & Metscher, B. (2022). Substantiating microCT for diagnosing bioerosion in archaeological bone using a new Virtual Histological Index (VHI). *Archaeological and Anthropological Sciences*, *14*, 104. https://doi.org/10.1007/s12520-022-01563-w

Margariti, E., Stathopoulou, E. T., Sanakis, Y., Kotopoulou, E., Pavlakis, P., & Godelitsas, A. (2019). A geochemical approach to fossilization processes in Miocene vertebrate bones from Sahabi, NE Libya. *Journal of African Earth Sciences*, *149*, 1–18. https://doi.org/10.1016/j.jafrearsci.2018.07.019

Mein, C., & Williams, A. (2023). Assessing the extent of bone bioerosion in short timescales. A novel approach for quantifying microstructural

loss. *Quaternary International*, *660*, 65–74. https://doi.org/10.1016/j.quaint.2023.01.011

Monasterio-Guillot, L., Crespo-López, L., Rodríguez Navarro, A. B., & Álvarez-Lloret, P. (2022). Comparative study of the mineralogy and chemistry properties of elephant bones: Implications during diagenesis processes. *Minerals*, *12*(11), 1384. https://doi.org/10.3390/min12111384

Nielsen-Marsh, C., Gernaey, A., Turner-Walker, G., Hedges, R., Pike, A. W. G., & Collins, M. (2000). The chemical degradation of bone. In M. Cox & S. Mays (Eds.), *Human Osteology* (pp. 439–454). Cambridge University Press.

Nielsen-Marsh, C. M., & Hedges, R. E. M. (2000). Patterns of diagenesis in bone I: The effects of site environments. *Journal of Archaeological Science*, *27*, 1139–1150. https://doi.org/10.1006/jasc.1999.0537

Pfretzschner, H.-U. (2004). Fossilization of Haversian bone in aquatic environments. *Comptes Rendus Palevol*, *3*, 605–616. https://doi.org/10.1016/j.crpv.2004.07.006

Pfretzschner, H.-U., & Tütken, T. (2011). Rolling bones—Taphonomy of Jurassic dinosaur bones inferred from diagenetic microcracks and mineral infillings. *Palaeogeography Palaeoclimatology Palaeoecology*, *310*(1–2), 117–123. https://doi.org/10.1016/j.palaeo.2011.01.026

Reiche, I., Lebon, M., Chadefaux, C., Müller, K., Le Hô, A.-S., Gensch, M., & Schade, U. (2010). Microscale imaging of the preservation state of 5,000-year-old archaeological bones by synchrotron infrared microspectroscopy. *Analytical and Bioanalytical Chemistry*, *397*, 2491–2499. https://doi.org/10.1007/s00216-010-3795-4

Reiche, I., Vignaud, C., & Menu, M. (2002). The crystallinity of ancient bone and dentine: New insights by transmission electron microscopy. *Archaeometry*, *44*, 447–459. https://doi.org/10.1111/1475-4754.00077

Ren, C., Li, Y.-F., Zhou, Q., & Li, W. (2021). Phosphate uptake by calcite: Constraints of concentration and pH on the formation of calcium phosphate precipitates. *Chemical Geology*, *579*, 120365. https://doi.org/10.1016/j.chemgeo.2021.120365

Rogoz, A., Sawlowicz, Z., & Wojtal, P. (2012). Diagenetic history of woolly mammoth (Mammuthus primigenius) skeletal remains from the archaeological site Cracow Spadzista street (B), Southern Poland. *PALAIOS*, *27*, 541–549. https://doi.org/10.2307/41692729

Schindelin, J., Arganda-Carreras, I., Frise, E., Kaynig, V., Longair, M., Pietzsch, T., Preibisch, S., Rueden, C., Saalfeld, S., Schmid, B., Tinevez, J. Y., White, D. J., Hartenstein, V., Eliceiri, K., Tomancak, P., & Cardona, A. (2012). Fiji: An open-source platform for biological-image analysis. *Natural Methods*, *9*(7), 676–682. https://doi.org/10.1038/nmeth.2019

Smith, C. I., Nielsen-Marsh, C. M., Jans, M. M. E., Arthur, P., Nord, A. G., & Collins, M. J. (2002). The strange case of Apigliano: Early 'fossilization' of medieval bone in southern Italy. *Archaeometry*, *44*, 405–415. https://doi.org/10.1111/1475-4754.t01-1-00073

Smith, C. I., Nielsen-Marsh, C. M., Jans, M. M. E., & Collins, M. J. (2007). Bone diagenesis in the European Holocene I: Patterns and mechanisms. *Journal of Archaeological Science*, *34*, 1485–1493. https://doi.org/10.1016/j.jas.2006.11.006

Tibbett, M., & Carter, D. O. (2008). *Soil analysis in forensic taphonomy*. CRC Press. https://doi.org/10.1201/9781420069921

Tripp, J. A., Squire, M. E., Hedges, R. E. M., & Stevens, R. E. (2018). Use of micro-computed tomography imaging and porosity measurements as indicators of collagen preservation in archaeological bone. *Palaeogeography Palaeoclimatology Palaeoecology*, *511*, 462–471. https://doi.org/10.1016/j.palaeo.2018.09.012

Trueman, C. N. (2013). Chemical taphonomy of biomineralized tissues. *Paleontology*, *56*(3), 475–486. https://doi.org/10.1111/pala.12041

Trueman, C. N., Privat, K., & Field, J. (2008). Why do crystallinity values fail to predict the extent of diagenetic alteration of bone mineral? *Palaeogeography Palaeoclimatology Palaeoecology*, *266*, 160–167. https://doi.org/10.1016/j.palaeo.2008.03.038

Trueman, C. N. G., Behrensmeyer, A. K., Tuross, N., & Weiner, S. (2004). Mineralogical and compositional changes in bones exposed on soil surfaces in Amboseli National Park, Kenya: Diagenetic mechanisms and the role of sediment pore fluids. *Journal of Archaeological Science*, *31*, 721–739. https://doi.org/10.1016/j.jas.2003.11.003

Trueman, C. N. G., & Martill, D. M. (2002). The long-term preservation of bone: The role of bioerosion. *Archaeometry*, *44*, 371–382. https://doi.org/10.1111/1475-4754.t01-1-00070

Turner-Walker, G. (2012). Early bioerosion in skeletal tissues: Persistence through deep time. *Neues Jahrbuch für Geologie und Paläontologie*, *265*(2), 165–183. https://doi.org/10.1127/0077-7749/2012/0253

Turner-Walker, G., Nielsen-Marsh, C. M., Syversen, U., Kars, H., & Collins, M. J. (2002). Sub-micron spongiform porosity is the major ultra-structural alteration occurring in archaeological bone. *International Journal of Osteoarchaeology*, *12*, 407–414. https://doi.org/10.1002/oa.642

Viani, A., Machová, D., Mácová, P., Mali, G., & Velemínský, P. (2021). Bone diagenesis in the medieval cemetery of Vratislavs' Palace in Prague. *Archaeological and Anthropological Sciences*, *13*, 39. https://doi-org.pros2.lib.unimi.it/10.1007/s12520-021-01286-4

Walden, S. J., Mulville, J., Rowlands, J. P., & Evans, S. L. (2018). An analysis of systematic elemental changes in decomposing bone. *Journal of Forensic Science*, *63*(1, 207–213. https://doi.org/10.1111/1556-4029.13480

Walkley, A., & Black, I. A. (1934). An examination of the Degtjareff method for determining soil organic matter, and proposed modification of the chromic acid titration method. *Soil Science*, *37*(1), 29–38. https://doi.org/10.1097/00010694-193401000-00003

White, L., & Booth, T. J. (2014). The origin of bacteria responsible for bioerosion to the internal bone microstructure: Results from experimentally-deposited pig carcasses. *Forensic Science International*, *239*, 92–102. https://doi.org/10.1016/j.forsciint.2014.03.024

Winer, S., & Bar-Yosef, O. (1990). States of preservation of bones from prehistoric sites in the Near East: A survey. *Journal of Archaeological Science*, *17*(2), 187–196. https://doi.org/10.1016/0305-4403(90)90058-D

Yan, J., Clifton, K. B., Mecholsky, J. J. Jr., & Gower, L. A. (2007). Effect of temperature on the fracture toughness of compact bone. *Journal of Biomechanics*, *40*, 1641–1645. https://doi.org/10.1016/j.jbiomech.2006.07.011

Young, R. A. (1993). *The Rietveld method*. Oxford University Press. https://doi.org/10.1093/oso/9780198555773.001.0001

SUPPORTING INFORMATION

Additional supporting information can be found online in the Supporting Information section at the end of this article.

How to cite this article: Caruso, V., Marinoni, N., Diella, V., Ferrari, E., Possenti, E., Trombino, L., Cattaneo, C., & Viani, A. (2024). A new laboratory-based method to experimentally induce diagenetic modifications in human bone tissue using archaeological gravesoils. *International Journal of Osteoarchaeology*, *34*(4), e3305. https://doi.org/10.1002/oa.3305